

**Combination of LEP-II results for the reaction
 $e^+e^- \rightarrow \gamma\gamma(\gamma)$ and interpretations.**

**The LEP Collaborations ALEPH, DELPHI, L3, OPAL,
The LEP-II Diphoton Working Group***

Abstract

This note presents a combination of published and preliminary results on the $e^+e^- \rightarrow \gamma\gamma(\gamma)$ reaction for the four LEP collaborations in preparation for the 2002 summer conferences. Averages in terms of deviations from the QED predictions for the total cross-section and the parameters obtained from differential cross-section fits are given. No deviations from the QED expectations have been found.

*The members of LEP-II Diphoton group are: J. Alcaraz, A. Bajo Vaquero, P. Checchia, P. Goncalves, K. Sachs, G. Taylor

1 Introduction

The reaction $e^+e^- \rightarrow \gamma\gamma(\gamma)$ provides a clean test of QED at LEP energies and is well suited to detect the presence of non-standard physics. The differential QED cross-section at the Born level in the relativistic limit is given by:

$$\left(\frac{d\sigma}{d\Omega}\right)_{\text{Born}} = \frac{\alpha^2}{s} \frac{1 + \cos^2\theta}{1 - \cos^2\theta}. \quad (1)$$

Since the two final state particles are identical the polar angle θ is defined such that $\cos\theta > 0$. Various models with deviations from this cross-section will be discussed in section 4. Results on the ≥ 2 -photon final state using the high energy data collected by the four LEP collaborations are reported by the individual experiments [1]. Here the results of the LEP working group dedicated to the combination of the $e^+e^- \rightarrow \gamma\gamma(\gamma)$ measurements are reported. Results are given for the averaged total cross-section and for global fits to the differential cross-sections.

2 Event Selection

This channel is very clean and the event selection, which is similar for all experiments, is based on the presence of at least two energetic clusters in the electromagnetic calorimeters. A minimum energy is required, typically $(E_1 + E_2)/\sqrt{s}$ larger than 0.3 to 0.6, where E_1 and E_2 are the energies of the two most energetic photons. In order to remove e^+e^- events, charged tracks are in general not allowed except when they can be associated to a photon conversion in one hemisphere.

The polar angle is defined in order to minimise effects due to initial state radiation as

$$\cos\theta = \left| \sin\left(\frac{\theta_1 - \theta_2}{2}\right) \right| / \sin\left(\frac{\theta_1 + \theta_2}{2}\right),$$

where θ_1 and θ_2 are the polar angles of the two most energetic photons. The acceptance in polar angle is in the range of 0.90 to 0.96 on $|\cos\theta|$, depending on the experiment.

With these criteria, the selection efficiencies are in the range of 68% to 98% and the residual background (from e^+e^- events and from $e^+e^- \rightarrow \tau^+\tau^-$ with $\tau^\pm \rightarrow e^\pm\nu\bar{\nu}$) is very small, 0.1% to 1%. Detailed descriptions of the event selections performed by the four collaborations can be found in [1].

3 Total cross-section

The total cross-sections are combined using a χ^2 minimisation. Given the different angular acceptances, only the ratios of the measured cross-sections relative to the QED expectation $r = \sigma_{\text{meas}}/\sigma_{\text{QED}}$ are averaged. Figure 1 shows the measured ratios $r_{i,k}$ of the experiments i at energies k with their statistical and systematic errors added in quadrature. There are no significant sources of experimental systematic errors that are correlated between experiments. The theoretical error on the QED prediction, which is fully correlated between energies and experiments is taken into account after the combination.

Denoting with Δ the vector of residuals between the measurements and the expected ratios, three different averages are performed:

1. per energy $k = 1, \dots, 7$: $\Delta_{i,k} = r_{i,k} - x_k$
2. per experiment $i = 1, \dots, 4$: $\Delta_{i,k} = r_{i,k} - y_i$
3. global value: $\Delta_{i,k} = r_{i,k} - z$

The seven fit parameters per energy x_k are shown in Figure 1 as LEP combined cross-sections. They are correlated with correlation coefficients ranging from 5% to 20%. The four fit-parameters per experiment y_i are uncorrelated between each other, the results are given in Table 1 together with the single global fit parameter z .

No significant deviations from the QED expectations are found. The global ratio is below unity by 1.8 standard deviations not accounting for the error on the radiative corrections (1%) which is of same size as the experimental error (1.0%).

Experiment	cross-section ratio
ALEPH	0.953 ± 0.024
DELPHI	0.976 ± 0.032
L3	0.978 ± 0.018
OPAL	0.999 ± 0.016
global	0.982 ± 0.010

Table 1: Cross-section ratios $r = \sigma_{\text{meas}}/\sigma_{\text{QED}}$ for the four LEP experiments averaged over all energies and the global average over all experiments and energies. The error includes the statistical and experimental systematic error but no error from theory.

4 Global fit to the differential cross-sections

The global fit is based on angular distributions at energies between 183 and 207 GeV from the individual experiments. As an example, angular distributions from each experiment are shown in Figure 2. Combined differential cross-sections are not available yet, since they need a common binning of the distributions. All four experiments give results including the whole year 2000 data-taking. Apart from the 2000 DELPHI data all inputs are final, as shown in Table 2. The systematic errors arise from the luminosity evaluation (including theory uncertainty on the small-angle Bhabha cross-section computation), from the selection efficiency and

	data used		sys. error [%]		cos θ
	published	preliminary	experimental	theory	
ALEPH	189 – 207	–	2	1	0.95
DELPHI	189 – 202	206	2.5	1	0.90
L3	183 – 207	–	2.1	1	0.96
OPAL	183 – 207	–	0.6 – 2.9	1	0.93

Table 2: The data samples used for the global fit to the differential cross-sections, the systematic errors, the assumed error on the theory and the polar angle acceptance for the LEP experiments.

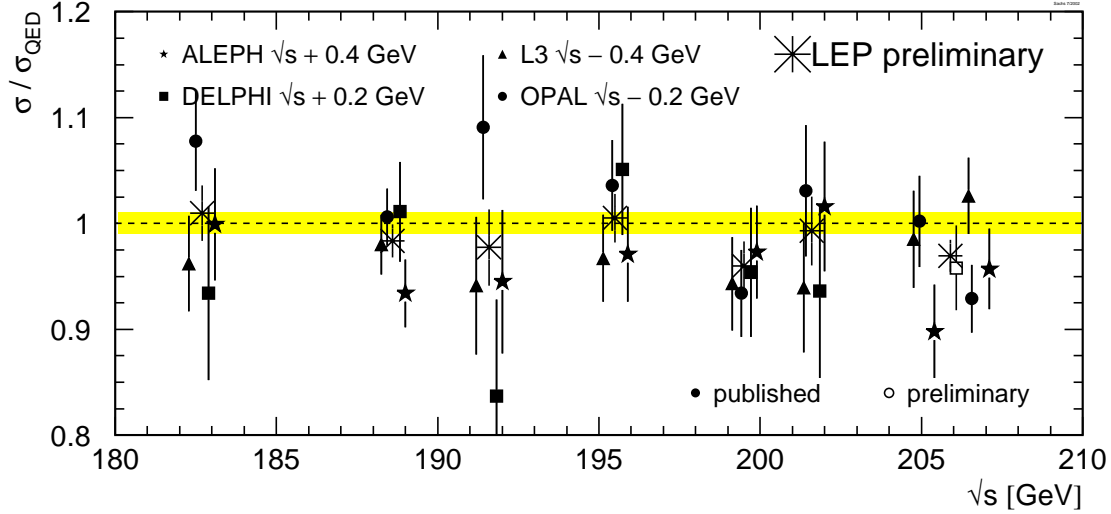


Figure 1: Cross-section ratios $r = \sigma_{\text{meas}}/\sigma_{\text{QED}}$ at different energies. The measurements of the single experiments are displaced by ± 200 or 400 MeV from the actual energy for clarity. Filled symbols indicate published results, open symbols stand for preliminary numbers. The average over the experiments at each energy is shown as a star. Measurements between 203 and 209 GeV are averaged to one energy point. The theoretical error is not included in the experimental errors but is represented as the shaded band.

the background evaluations and from radiative corrections. The last contribution, owing to the fact that the available $e^+e^- \rightarrow \gamma\gamma(\gamma)$ cross-section calculation is based on $\mathcal{O}(\alpha^3)$ code, is assumed to be 1% and is considered correlated among energies and experiments.

Various model predictions are fitted to these angular distributions taking into account the experimental systematic error correlated between energies for each experiment and the error on the theory. A binned log likelihood fit is performed with one free parameter for the model and five fit parameters used to keep the normalisation free within the systematic errors of the theory and the four experiments. Additional fit parameters are needed to accommodate the angular dependent systematic errors of OPAL.

The following models of new physics are considered. In some cases they give rise to identical distortions of the predictions; hence their parameters can be transformed from one to another.

Cut-off parameter Λ_{\pm} [2, 3]:

$$\left(\frac{d\sigma}{d\Omega}\right)_{\Lambda_{\pm}} = \left(\frac{d\sigma}{d\Omega}\right)_{\text{Born}} \pm \frac{\alpha^2 s}{2\Lambda_{\pm}^4} (1 + \cos^2 \theta) \quad (2)$$

Effective Lagrangian theory [4] describing anomalous $e^+e^-\gamma$ couplings in dimension 6 ($\Lambda_6^4 = \frac{2}{\alpha}\Lambda_{\pm}^4$) or contact interactions for dimensions 7 and 8 ($\Lambda_7 = \Lambda'$; $\Lambda_8^4 = m_e\Lambda_7^3$):

$$\left(\frac{d\sigma}{d\Omega}\right)_{\Lambda'} = \left(\frac{d\sigma}{d\Omega}\right)_{\text{Born}} + \frac{s^2}{32\pi\Lambda'^6} \quad (3)$$

Low scale gravity in extra dimensions [5], where M_s is related to the string scale and expected

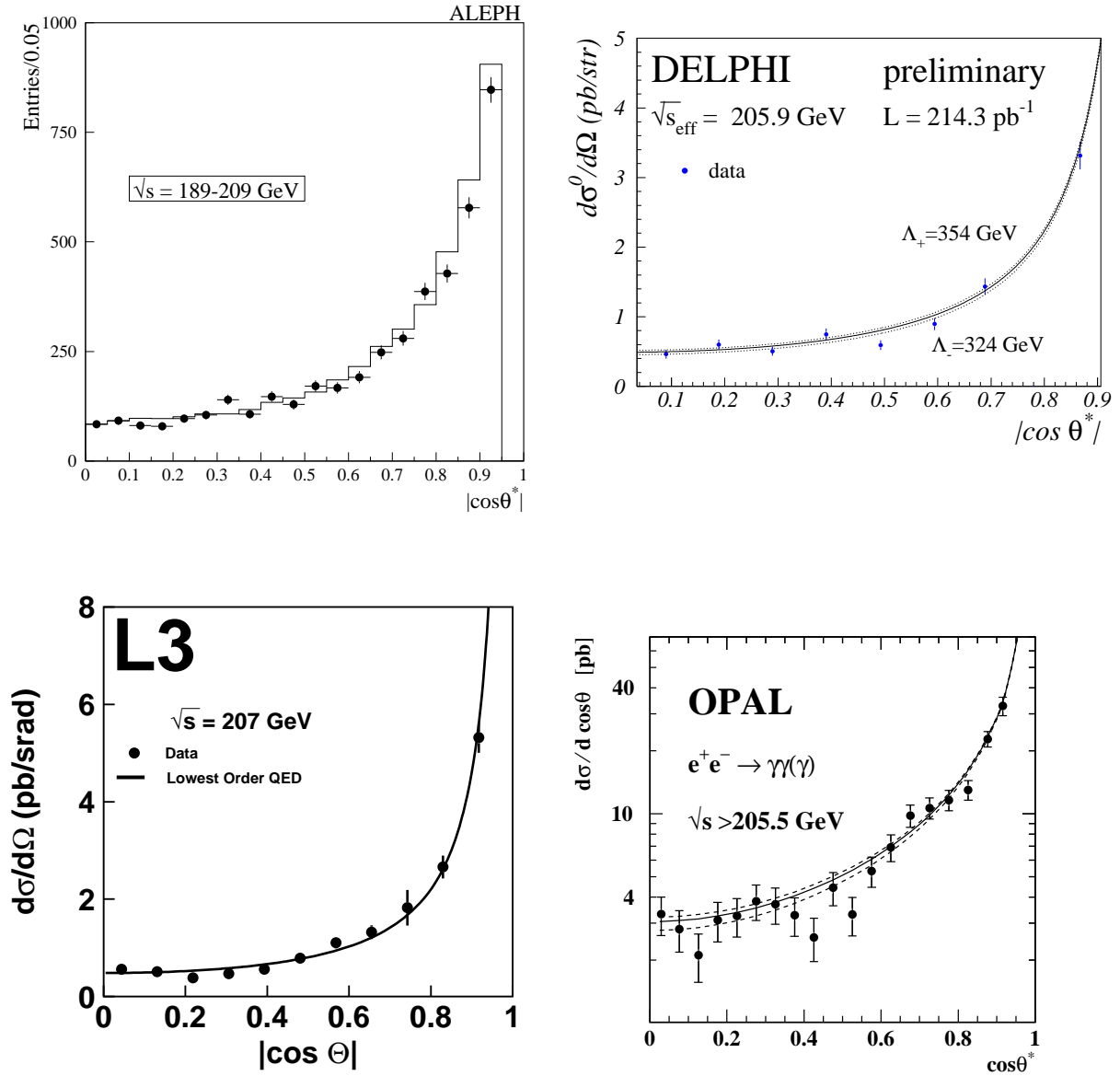


Figure 2: Examples for angular distributions of the four LEP experiments. Points are the data and the curves are the QED prediction (solid) and the individual fit results for Λ_{\pm} (dashed). ALEPH shows the uncorrected number of observed events, the expectation is presented as histogram.

to be of order $\mathcal{O}(\text{TeV})$:

$$\left(\frac{d\sigma}{d\Omega}\right)_{\text{Ms}} = \left(\frac{d\sigma}{d\Omega}\right)_{\text{Born}} - \frac{\alpha s}{2\pi} \frac{\lambda}{M_s^4} (1 + \cos^2 \theta) + \frac{s^3}{16\pi^2} \frac{\lambda^2}{M_s^8} (1 - \cos^4 \theta), \quad \lambda = \pm 1 \quad (4)$$

Excited electrons [6] with mass M_{e^*} and chiral magnetic coupling described by the Lagrangian

$$\mathcal{L} = \frac{1}{2\Lambda} \bar{\ell}^* \sigma^{\mu\nu} \left[g f \frac{\tau}{2} W_{\mu\nu} + g' f' \frac{Y}{2} B_{\mu\nu} \right] \ell_L + \text{h.c.}, \quad (5)$$

where g and g' are the coupling constants of $\text{SU}(2)_L$ and $\text{U}(1)_Y$, respectively. For the two photon final state this leads to the following cross-section:

$$\left(\frac{d\sigma}{d\Omega}\right)_{e^*} = \left(\frac{d\sigma}{d\Omega}\right)_{\text{Born}} + \frac{\alpha^2 f_\gamma^4}{4 \Lambda^4} M_{e^*}^2 \left[\frac{p^4}{(p^2 - M_{e^*}^2)^2} + \frac{q^4}{(q^2 - M_{e^*}^2)^2} + \frac{\frac{1}{2}s^2 \sin^2 \theta}{(p^2 - M_{e^*}^2)(q^2 - M_{e^*}^2)} \right], \quad (6)$$

with $f_\gamma = -\frac{1}{2}(f + f')$, $p^2 = -\frac{s}{2}(1 - \cos \theta)$ and $q^2 = -\frac{s}{2}(1 + \cos \theta)$ and $\Lambda = M_{e^*}$. Two kinds of fits are performed for the two model parameters M_{e^*} and f_γ .

5 Fit Results

Where possible the fit parameters are chosen such that the likelihood function is approximately Gaussian. The preliminary results of the fits to the differential cross-sections are given in Table 3. No significant deviations with respect to the QED expectations are found (all the parameters are compatible with zero) and therefore 95% confidence level limits are obtained by renormalising the probability distribution of the fit parameter to the physically allowed region. The asymmetric limits x_{95}^\pm on the fitting parameter are obtained by:

$$\frac{\int_0^{x_{95}^+} \Gamma(x, \mu, \sigma) dx}{\int_0^\infty \Gamma(x, \mu, \sigma) dx} = 0.95 \quad \text{and} \quad \frac{\int_{x_{95}^-}^0 \Gamma(x, \mu, \sigma) dx}{\int_{-\infty}^0 \Gamma(x, \mu, \sigma) dx} = 0.95, \quad (7)$$

where Γ is a Gaussian with the central value and error of the fit result denoted by μ and σ , respectively. This is equivalent to the integration of a Gaussian probability function as a function of the fit parameter. The 95 % CL limits on the model parameters are derived from the limits on the fit parameters, e.g. the limit on Λ_+ is obtained as $[x_{95}^+(\Lambda_\pm^{-4})]^{-1/4}$. For limits on f_γ/Λ a scan over M_{e^*} is performed and presented in Figure 3. In the case of the excited electron mass the fit cannot be expressed in terms of a linear fit parameter. The curve of the negative log likelihood, ΔLogL , is shown in Figure 4. The value corresponding to $\Delta\text{LogL} = 1.92$ is $M_{e^*} = 248$ GeV.

6 Conclusion

The LEP collaborations study the $e^+e^- \rightarrow \gamma\gamma(\gamma)$ channel up to the highest available centre-of-mass energies. The total cross-section results are combined in terms of the ratios with respect to the QED expectations. No deviations are found. The differential cross-sections are fit following different parametrisations from models predicting deviations from QED. No evidence for deviations is found and therefore combined 95% confidence level limits are given.

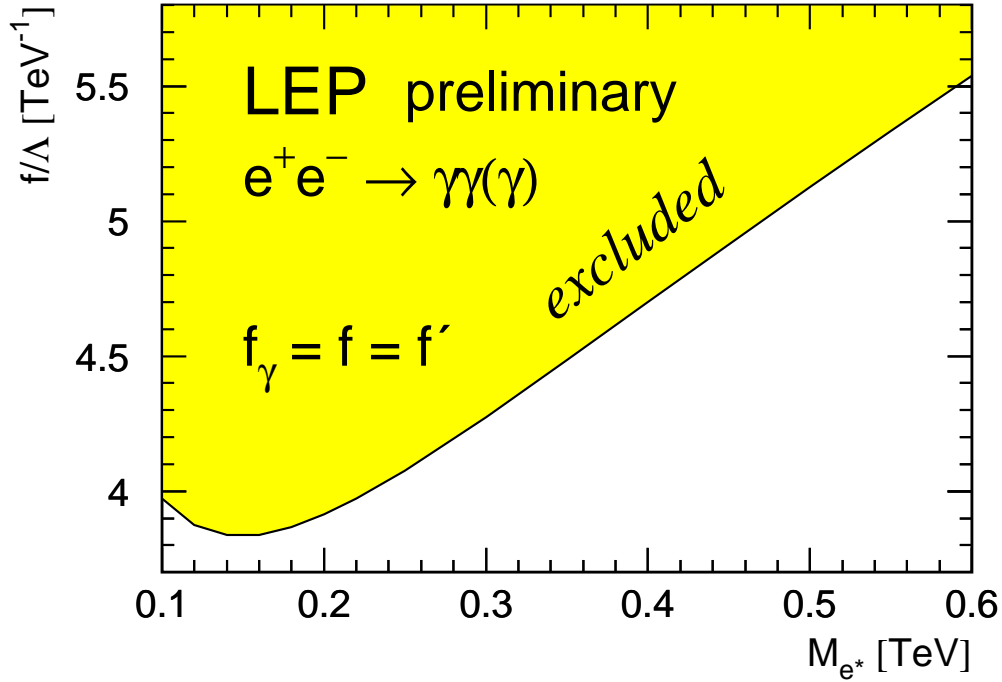


Figure 3: 95% CL limits on f_γ/Λ as a function of M_{e^*} . In the case of $f = f'$ it follows that $f_\gamma = f$. It is assumed that $\Lambda = M_{e^*}$.

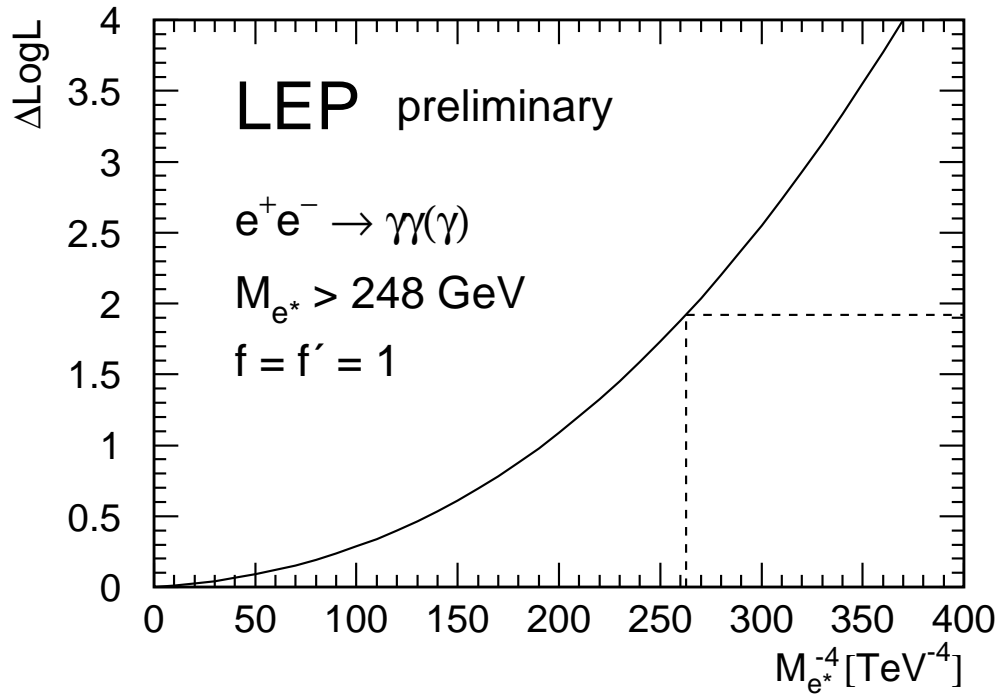


Figure 4: Log likelihood difference $\Delta\text{LogL} = -\ln \mathcal{L} + \ln \mathcal{L}_{\text{max}}$ as a function of $M_{e^*}^{-4}$. The coupling is fixed at $f = f' = 1$. The value corresponding to $\Delta\text{LogL} = 1.92$ is $M_{e^*} = 248 \text{ GeV}$.

Fit parameter	Fit result	95% CL limit [GeV]
Λ_{\pm}^{-4}	$(-12.5^{+25.1}_{-24.7}) \cdot 10^{-12} \text{ GeV}^{-4}$	$\Lambda_+ > 392$ $\Lambda_- > 364$
Λ_7^{-6}	$(-0.91^{+1.81}_{-1.78}) \cdot 10^{-18} \text{ GeV}^{-6}$	$\Lambda_7 > 831$
	derived from Λ_+	$\Lambda_6 > 1595$
	derived from Λ_7	$\Lambda_8 > 23.3$
λ/M_s^4	$(0.29^{+0.57}_{-0.58}) \cdot 10^{-12} \text{ GeV}^{-4}$	$\lambda = +1: M_s > 933$ $\lambda = -1: M_s > 1010$
$f_{\gamma}^4(M_{e^*} = 200\text{GeV})$	$0.037^{+0.202}_{-0.198}$	$f_{\gamma}/\Lambda < 3.9 \text{ TeV}^{-1}$

Table 3: The preliminary combined fit parameters and the 95% confidence level limits for the four LEP experiments.

References

- [1] ALEPH Collab., CERN-EP/2002-033 and ref. therein;
DELPHI Collab., DELPHI 2001-093 CONF 521 and ref. therein;
L3 Collab., Phys. Lett. **B531** (2002) 28 and ref. therein;
OPAL Collab., *Multi-Photon Production in e^+e^- Collisions at $\sqrt{s} = 181 - 209 \text{ GeV}$* , CERN-EP/2002-xxx
- [2] S. D. Drell, Ann. Phys. **4** (1958) 75
- [3] F. E. Low, Phys. Rev. Lett. **14** (1965) 238
- [4] O. J. P. Eboli, A. A. Natale, and S. F. Novaes, Phys. Lett. **B271** (1991) 274
- [5] K. Agashe and N. G. Deshpande, Phys. Lett. **B456** (1999) 60
- [6] B. Vachon, *Excited electron contribution to the $e^+e^- \rightarrow \gamma\gamma$ cross-section*, hep-ph/0103132, 2001